



Advanced magnetic resonance imaging (MRI) of soft tissue tumors: techniques and applications

Federico Bruno¹ · Francesco Arrigoni¹ · Silvia Mariani¹ · Alessandra Splendiani¹ · Ernesto Di Cesare¹ · Carlo Masciocchi¹ · Antonio Barile¹ 

Received: 11 April 2018 / Accepted: 29 March 2019 / Published online: 4 April 2019
© Italian Society of Medical Radiology 2019

Abstract

Imaging evaluation of soft tissue tumors is important for the diagnosis, staging, and follow-up. Magnetic resonance imaging (MRI) is the preferred imaging modality due to its multiplanarity and optimal tissue contrast resolution. However, standard morphological sequences are often not sufficient to characterize the exact nature of the lesion, addressing the patient to an invasive bioptic examination for the definitive diagnosis. The recent technological advances with the development of functional MRI modalities such as diffusion-weighted imaging, dynamic contrast-enhanced perfusion imaging, magnetic resonance spectroscopy, and diffusion tensor imaging with tractography have implemented the multiparametricity of MR to evaluate in a noninvasive manner the biochemical, structural, and metabolic features of tumor tissues. The purpose of this article is to review the state of the art of these advanced MRI techniques, with focus on their technique and clinical application.

Keywords MRI · Soft tissue tumors · DWI · Spectroscopy · DTI

Introduction

Soft tissue tumors (STT) that include a large variety of benign and malignant lesions are of a diverse histological nature. Incidence increases with age and is higher in males: Benign lesions have an incidence of approximately 300/100,000, while malignant ones (that account for 1% of all malignant tumors) about 5/10,000 per year. The prognosis of these diseases depends on a correct and early diagnosis, the efficacy of treatment, and accurate follow-up for monitoring of recurrence [1]. Beyond the clinical evaluation, imaging plays a fundamental role in the initial assessment of soft tissue tumors for a cost-effective patient management, and MR imaging is considered the modality of choice due to its intrinsic high tissue contrast and multiplanarity, as in the study of other pathologies in the musculoskeletal field [1–10]. With the use of standard pulse sequences, it is possible to evaluate the signal intensity, growth pattern, degree of enhancement, and relationship with neighboring

anatomical structures [11]. Standard protocols should include T1- and T2-weighted sequences, with and without fat saturation, gradient echo sequences (detection of hemorrhage), and post-contrast acquisitions, in at least two orthogonal planes [12, 13]. However, using standard morphological sequences alone, few soft tissue lesions have specific and pathognomonic MR characteristics (e.g., simple lipoma/cyst, hemangioma), and the differential diagnosis remains very wide for most cases; another problem is to differentiate a benign histotype from a malignant, also often not immediate with standard imaging as some overlap exists [14–17]. The literature data report conflicting results on the diagnostic accuracy of MRI in identifying the lesion histotype, with results varying from 25% to 90% [18]. However, the gold standard to assess tumor type and grade is histopathology, which requires an invasive bioptic approach [19]. Many limitations of the standard MR sequences are also encountered in the follow-up, both in assessing the response to radio-chemotherapy treatment and in identifying possible residual and recurrent tumor after surgery [13]. In recent years, there has been an increased technical advancement in functional MR sequences, such as proton (1H) magnetic resonance spectroscopy (MRS), diffusion-weighted MRI (DWI), and dynamic contrast-enhanced (DCE) MRI. These sequences provide detailed structural and metabolic information about

✉ Antonio Barile
antonio.barile@cc.univaq.it

¹ Department of Biotechnology and Applied Clinical Sciences, S. Salvatore Hospital, University of L'Aquila, Vetoio Street, 1, 67100 L'Aquila, Italy

tumor tissue, allowing to formulate a diagnostic hypothesis as close as possible to histological diagnosis in a noninvasive way [13, 20–23].

The purpose of this article is to review technical aspects of each of these advanced MR imaging techniques, with a particular focus on their clinical application in the characterization, differentiation of benign from malignant lesions and the assessment of response to treatment in soft tissue tumors.

Diffusion-weighted imaging (DWI)

DWI is a functional MRI technique that provides information about tissue cellularity and cell membrane integrity, evaluating the diffusivity of water molecules (Brownian motion) [24–27].

Technique

The DWI signal is given by the degree of movement of water molecules in cellular spaces (extracellular, intracellular, transcellular, and intravascular), in an inversely proportional manner [28]. The movement of water molecules is restricted in high-cellularity tissues, intact cell membranes, and reduced extracellular spaces. On the contrary, in tissues with low cellularity and considerable extracellular spaces, the movement of the water molecules is facilitated [11]. It is important to take into account the contribution to the DWI signal of the intravascular movement of water molecules since in very vascularized lesions it can be significant [1, 11, 19].

There are several DWI sequences, including spin-echo DWI, echo-planar imaging (EPI), and steady-state free precession sequences [11]. The most used is the single or multishot EPI, less sensitive to motion artifact and with shorter acquisition times. The acquisition must provide at least two b values to calculate the apparent diffusion coefficient (ADC). Generally, values of 50, 400, and 1000 s/mm² are used, but the parameters are variable in the various institutions [15]. The ADC is expressed as a parametric map and can be evaluated qualitatively or quantitatively through the positioning of region of interest (ROI). There is no standardization on the number and size of the ROI to be placed, nor on the evaluation of the mean, minimum or maximum ADC. Some authors suggest that the evaluation of the minimum ADC may be more accurate as it would represent the area of the greatest cellularity of the lesion [11, 29]. As mentioned earlier, it is important to take into account tissue perfusion and intravascular water component, as ADC values increase in vascularized tumors, leading to overlapping in ADC values between benign and malignant tumors. To avoid this, it is possible to use perfusion-insensitive ADC values (PIADC) [13, 29]. The main limits of DWI are represented by the

inherent low signal-to-noise ratio and by the low spatial resolution, the artifacts from susceptibility (artifacts in correspondence of tissues with blood products or air). For these reasons, DWI must always be interpreted in conjunction with anatomical sequences [15, 19, 29, 30].

Applications

The DWI signal and the ADC values reflect the cellularity of the tissues, so even if there are no normal cutoff values, DWI can characterize the biological activity of the tissues. In the study of musculoskeletal soft tissue tumors, this means that, as a general rule, benign tumors with a low degree of biological activity will have a loss of ADC signal as the b values increase, while malignant tumors (in which the water has greater restriction in movement) will show high intensity at high b values. The results of the use of DWI in the characterization of the nature of the lesions are numerous in the literature. Pekcevik et al. [31] found that the mean ADC values of benign and malignant soft tissue tumors were statistically different, with values of 2.31 ± 1.29 and 0.90 ± 0.70 , respectively. The authors found the highest values in benign cystic tumors and the lowest values in giant cell tumors of tendon sheaths (maybe due to their spindle-shaped stromal cells' and multinucleated giant cells' histological composition). Joung et al. [30], using conventional MRI and DWI sequences together, obtained values of sensitivity, specificity, and accuracy of 96%, 85.7%, and 90%, respectively. The authors confirmed the persistence of high signal intensity with increasing b values in all malignant lesions (muscular metastases, myxoid liposarcoma, etc.) on the qualitative evaluation, with low ADC values on quantitative analysis with increasing b values, although with differences among the various histological types. They also found that higher b values (more than 800 s/mm²) are useful to increase the contrast between benign and malignant lesions and thus reduce the number of equivocal cases. All benign myxoid lesions showed loss of high signal intensity with increasing b values (e.g., schwannoma).

Some authors [11, 19] suggested that in highly necrotic lesions the surrounding edema may contaminate tumor tissue and increase the diffusion coefficient.

Demehri et al. [32] reported the role of DWI in the distinction between *benign and malignant peripheral nerve sheath tumors*; in particular, their results showed that the minimum ADC value is a better indicator of malignancy than the average ADC value, due to the heterogeneity in cellularity of both benign and malignant PNSTs. Moreover, in the planning of image-guided biopsies, targeting areas with the lowest ADC values can improve the diagnostic yield [23]. In their study, the same authors found that benign neurofibromas showed high minimum apparent

diffusion coefficient (ADC) values ($> 1.1 \times 10^{-3} \text{ mm}^2/\text{s}$), as well as schwannomas (> 1.1 to $1.2 \times 10^{-3} \text{ mm}^2/\text{s}$).

DWI is also particularly useful to *distinguish cystic from solid lesions* without the use of contrast administration, with high negative predictive value for ruling out a tumor, being an ADC value greater than $2.5 \times 10^{-3} \text{ mm}^2/\text{s}$ suggestive of a benign cystic lesion (sensitivity of 80% and a specificity of 100%) [15] (Fig. 1).

The evaluation of *myxoid tumors* with DWI must be performed with particular attention; this is because myxoid tumors due to their high mucin and low collagen contents have higher diffusion coefficients than nonmyxoid tumors.

According to the results of Young et al. [33], ADC value is less useful for discriminating between benign and malignant lesions in case of myxoid lesions, as the difference in ADC values was not statistically significant [15, 22, 23].

Similarly, both benign and aggressive *fatty tumors* have very low ADC values, and ADC values of these lesions are not comparable with those of nonfatty tumors [13].

In *vascular tumors*, DWI is influenced by tumor perfusion, and the value of ADC analysis in these lesions is still to be determined [13].

Oka et al. [34] evaluated the feasibility of DWI in differentiating *chronic expanding hematomas (CEH)* from hemorrhagic soft tissue tumors. They found that the mean ADC value of CEH was significantly higher than that of malignant soft tissue tumors.

Gasparetto et al. [11] found that also *myositis ossificans* shows facilitated diffusion on DWI and high ADC values, findings consistent with a benign tumor. So evaluating the clinical history and implementing imaging with DWI, they suggested a follow-up examination after 2–4 weeks to confirm the diagnosis, so avoiding unnecessary biopsy.

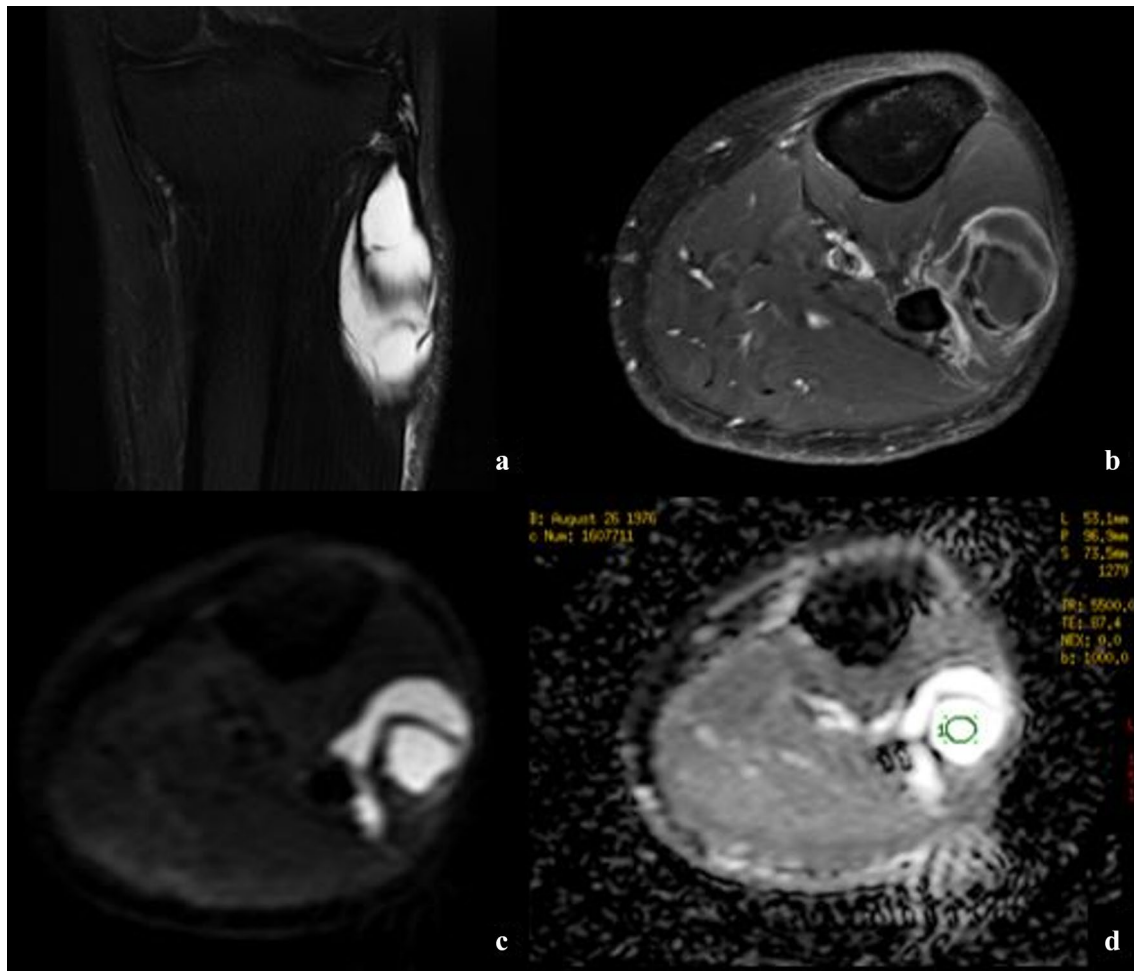


Fig. 1 Coronal and axial MR images of a cystic soft tissue lesion at the level of the proximal leg. The lesion shows homogeneous internal fluid signal intensity with peripheral contrast enhancement, features suggestive for a perineural ganglion cyst of the common peroneal nerve.

DWI sequences show values of $2.75 \times 10^{-3} \text{ mm}^2/\text{s}$ (b value = 1000) on ADC map, confirming the benign cystic nature of the lesion

In another study [28], mean ADC of *desmoid tumors* was found to be significantly higher than that of malignant soft tissue tumors without overlap in the minimum ADC values.

DWI has proved very useful also in the *assessment of treatment response* to chemotherapy in soft tissue tumors. In fact, changes in tumor size with standard MRI imaging are not a useful criterion as in other solid tumors [15]. Similarly, the evaluation of enhancement patterns can be challenging, as both granulation and scar tissues (aspecific tissue changes after chemo/radiotherapy) are enhancing after contrast administration, and the differentiation from the viable tumor is not always direct [15]. DWI demonstrated to improve this discrimination earlier than conventional imaging, as solid tumors are characterized by high cellularity with intact cell membranes, while tissues after cytotoxic treatment show lower cellularity and membrane damage [15, 22]. DWI implements standard morphological sequences also in the evaluation of postsurgical follow-up [6, 35, 36], aiding to detect residual/recurrent tumor tissue.

Dynamic perfusion MRI

Dynamic perfusion MRI is a functional imaging technique often used to evaluate musculoskeletal tumors, mainly to depict early intravascular and interstitial distribution of gadolinium [22, 29, 37].

Technique

DCE-MRI is typically performed with multiple repeated rapid, volumetric, and gradient echo sequences acquired immediately after intravenous administration of gadolinium. At our institution, routine dynamic contrast enhancement is performed using T1 3 double fast spin-echo (DFSE) sequences with fat saturation [29]. After an initial baseline scan identifying the best plane for lesion visualization and performing, we administer a bolus of gadolinium (0.1 mmol/kg). We then perform eight 19-s scans in fast succession, with a scan delay variable on the region to be studied but that never exceeding 20 s, to ensure proper arterial-phase perfusion. Then, a last scan is performed 5 min after contrast administration. Similar to DWI, DCE-MRI can also be analyzed qualitatively or quantitatively [13, 29]. Qualitative analysis is performed comparing tumor enhancement with arterial enhancement. Although widely available, this method is somewhat subjective hampering data comparison and the establishment of general diagnostic criteria. It provides a fairly reliable method for the identification of early tumor enhancement, which tends to be associated with malignancy [13]. Semiquantitative methods of postprocessing involve the postprocessing of time–intensity curves using three identical ROIs positioned at a site of marked early

tumor enhancement, in an artery, and in a healthy muscle, respectively [22, 37, 38]. The resulting time–intensity curves provide a graphic representation of contrast perfusion, from which quantitative information (time to enhancement, wash in, peak enhancement, and washout) can be obtained [37].

The curves can be classified into five types [22]:

- type 1, no enhancement (e.g., lipoma);
- type 2, weak and gradual enhancement (e.g., benign tumors or schwannoma);
- type 3, rapid early enhancement followed by a plateau (e.g., benign vascular tumors, desmoid tumors, abscesses, and some malignant tumors, but with limited specificity);
- type 4, rapid early enhancement followed washout (highly vascular tumors with small interstitial compartment such as malignant histiocytofibroma, synovial sarcoma, and leiomyosarcoma and several benign tumors such as giant cell tumor);
- type 5, rapid early enhancement followed by slow, gradual enhancement (tumors with large interstitial compartments such as myxoid tumors).

However, even if malignant lesions typically demonstrate rapid early arterial enhancement and higher slopes of enhancement compared with benign lesions, the patterns may show some degree of overlap secondary to highly vascularized benign lesions and poorly vascularized or necrotic malignant lesions [29].

Applications

The main applications in the imaging of soft tissue tumors of dynamic perfusion MRI are in the characterization of the lesions, identification of viable tumor areas to target biopsy, monitoring of chemotherapy treatment outcome, and differentiation of residual tumor from scarring [11, 22, 39]. DCE-MRI differentiates benign and malignant lesions on the base of the different enhancement rates, an index of lesion vascularity, and perfusion. Van Rijswijk et al. [40] determined that dynamic contrast-enhanced imaging was significantly superior to both unenhanced imaging and static contrast-enhanced imaging in the prediction of malignancy. In the authors' previous experience, we identified different curves between lesions with the different biological aggressiveness in both bone and soft tissue tumors [37]. Regarding soft tissue lesions, whereas perfusion MRI enabled differentiation between lesions with low and high biological aggressiveness, we could never obtain typical time–intensity curves for the various histological tumor types [37]. Analysis of the slope of the time–intensity curves proved to be a sensible and specific indicator (64–58%) in determining the biological aggressiveness of soft tissue lesions [37] (Fig. 2).

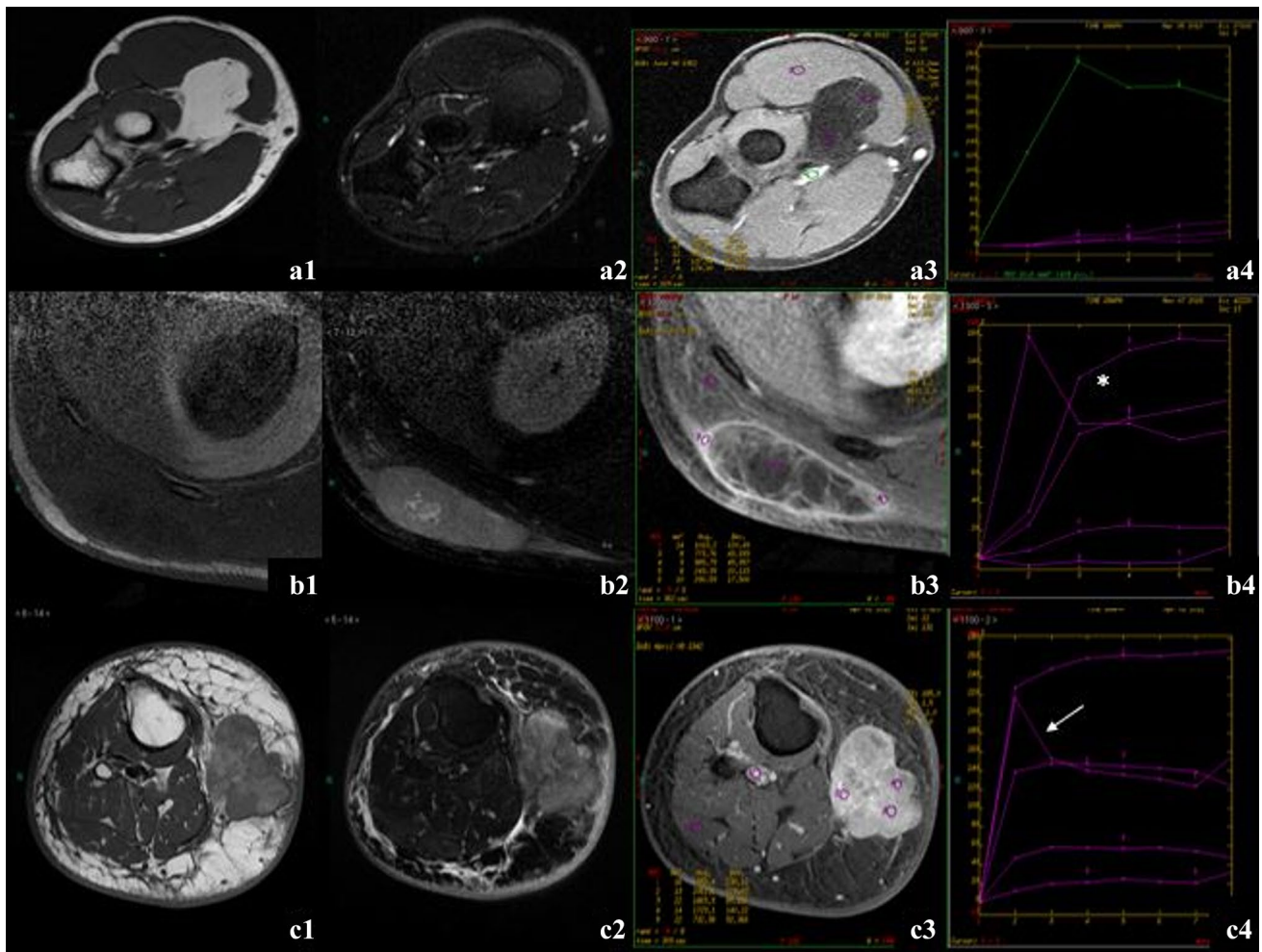


Fig. 2 MRI axial images of three different lesions with dynamic perfusion study. Pictures **a**₁₋₄: lipoma of the elbow showing homogeneous hyperintense signal intensity on a T1-weighted sequence (**a**₁) and no enhancement on qualitative evaluation after gadolinium administration (**a**₂). Evaluation of time–intensity curves with ROI positioning (**a**₃, **a**₄) shows a type 1 curve, conforming the benign nature of the lesion. The second subcutaneous lesion (**b**₁₋₄) shows inhomogeneous internal structure with areas of adipose signal intensity, intralesional

septa, and prevalent peripheral enhancement after gadolinium injection (**b**₃), with evidence of a type 2 signal intensity curve. Cases **c**₁₋₄ show a subcutaneous polilobulated lesion of the leg strictly adherent to the superficial fascia, with inhomogeneous internal structure and intense contrast enhancement after gadolinium injection (**c**₄), with evidence of time–intensity curves types 3 and 4 (arrow). The MRI features of the lesion are consistent with a myxoid liposarcoma

On dynamic contrast-enhanced MR imaging, *malignant peripheral nerve sheath tumors* (MPNSTs) usually show early arterial enhancement that is much rarer in their benign counterpart (BPNSTs) [23].

The application of dynamic perfusion MRI in *guiding bioptic procedures* is particularly useful in soft tissue tumors that have a significant “cystic” or hemorrhagic component [1, 41], as purely fluid areas without contrast enhancement should be avoided during biopsy, to prefer the more solid, enhanced portions. Dynamic contrast-enhanced MRI is also helpful in delineating *tumor margins*; in fact, tumor enhancement is precocious and faster than that of peritumoral edema and the initial slopes of tumor and nontumor tissues differ significantly [11].

Perfusion MRI is also useful for *distinguishing cysts from myxoid tumors* and to characterize the benign or malignant nature of myxoid lesions: Cysts show no enhancement, while the myxoid component of sarcomas exhibits early and avid enhancement [11]. Matching the findings of morphological sequences, DWI/ADC values, perfusion, and spectroscopy improve the diagnostic accuracy in myxoid tumors [22].

Ohgiya et al. [42] evaluated the role of dynamic contrast-enhanced MR imaging in the diagnosis of *vascular malformations (VMs)* with high specificity [43]. They showed that low-flow vascular malformations, mainly VMs, had a contrast rise time ranging between 50 and 100 s with a mean of 88.4 s. This was significantly higher than the “contrast rise time” results of high-flow vascular malformations (less

than 20 s in all lesions with a mean of 5.8 s). The authors postulated that whether differentiation of low-flow from high-flow vascular malformations can be made with nearly 100% sensitivity and specificity setting a 30-s threshold for the “contrast rise time” [43].

Dynamic enhancement is also showing utility in monitoring chemotherapy response, evaluating the degree of tumor necrosis and distinguishing postoperative tissue changes (e.g., fibrosis) from recurrent tumor [1]. Direct visual (qualitative) inspection of MRI images allows simple recognition of perfused viable tumor tissue with less intense (slower enhancing) areas of peritumoral edema, normal tissue, and tumor necrosis [11]. The presence of more than 10% of viable tumor tissue indicates a poor response to treatment. In these patients, early enhancement images are useful for guiding a new biopsy or for suggesting histological confirmation of a particular area in the resected specimen. Quantitatively, an at least 60% decrease in the time–intensity curve slope value indicates more than 90% of tumor necrosis and good treatment outcome [11, 22]. The reported diagnostic accuracy for differentiating good and poor treatment response in the literature ranges from 85.7 to 100%. Optimal follow-up requires three dynamic perfusion MRI studies: preoperatively (before the biopsy and before surgery) and postoperatively (during chemotherapy) [11]. In soft tissue sarcomas, strongly enhancing foci represent residual or recurrent tumor, while the absence of early enhancement indicates good treatment response. Follow-up examinations (after 3–6 months) are necessary when evaluating the treatment response after radiotherapy, as radiotherapy may lead to granulation tissue with increased perfusion that cannot be distinguished by residual tumor early [22].

Magnetic resonance spectroscopy (MRS)

MRS is a functional noninvasive imaging technique that requires no intravenous contrast administration and characterizes lesions based on their metabolic constituents [1, 11, 13, 29, 44]. Different metabolites can be observed depending on the MRS technique. Phosphorus-31 (31P) MRS evaluates metabolites containing phosphorus such as phosphocreatine, inorganic phosphate, and ATP. Though MRS with 31 P has demonstrated potential for the evaluation of musculoskeletal masses, and it requires specialized MRI hardware, which limits its clinical feasibility. Proton (1H) MRS is more easily integrated into clinical practice as it requires no specialized equipment.

Technique

Clinical MRS can be performed either at 1.5T or at 3T. Higher field strengths provide a greater signal-to-noise ratio

(SNR), with improved spectral resolution; the main drawbacks are the increased field inhomogeneity and the consequently increased metabolite line widths [44]. Single-voxel technique or a multi-voxel technique can be used for proton MRS. The single-voxel technique is a simple, time-effective approach that provides good magnetic field homogeneity within the volume of interest. Using the multi-voxel technique, it is possible to obtain information over a wider field of view, analyzing entire large lesions and surrounding tissue or multiple lesions with a single acquisition. Multi-voxel images, on the other hand, take longer scan times and are more technically challenging. However, most authors prefer mono-voxel spectroscopy over multi-voxel technique in MSK spectroscopy [7]. MRS evaluation may be either qualitative or quantitative. The qualitative analysis evaluates the presence or absence of a specific metabolite peak, but may be burdened by false positive results. Quantitative evaluation is thus generally preferred. Values can be obtained measuring the peak ratio between metabolites or between a metabolite and the background noise level (SNR). The positioning of ROIs is critical to avoid areas containing bony structures, necrotic or hemorrhagic foci (underestimation of the choline peak), calcifications (increased field inhomogeneity), fat (can obscure the choline peaks), or muscle (overestimation of the choline peak). The enhancing portion of the tumor is targeted in ROI positioning; for tumors exhibiting weak/slow enhancement or no enhancement after 5 min, the voxel is positioned at sites of delayed enhancement [44].

Applications

Already widely used in neuroradiology, magnetic resonance spectroscopy (MRS) has recently gained also a role in the musculoskeletal field. One of the main applications is the assessment of malignancy in musculoskeletal tumors since specific metabolites (trimethylamine/choline-containing compounds including phosphocholine, glycerophosphocholine, and free choline) are distinctively increased in malignant lesions, and they are considered as a marker of malignancy [45]. To date, the literature results in musculoskeletal MRS investigated the qualitative analysis of the choline or trimethylamine peak as a marker for malignancy [21, 44]. Doganay et al. [4] obtained a sensitivity of 72.2%, specificity of 83.3%, and an accuracy of 76.6% in detecting malignant bone and soft tissue tumors. In another group [5], sensitivity and specificity were 95% and 83%, respectively. They concluded that the absence of choline peak is highly predictive of benign tumors and that 1H-MRS is a feasible approach to differentiate malignant from benign tumors (Fig. 3). In a series of Russo et al., all tumors with a mitotic index greater than 2/10 HPF had a positive choline peak and were malignant and correlation between 1H-MRS findings and mitotic index was high [16]. However, some benign tumors show a

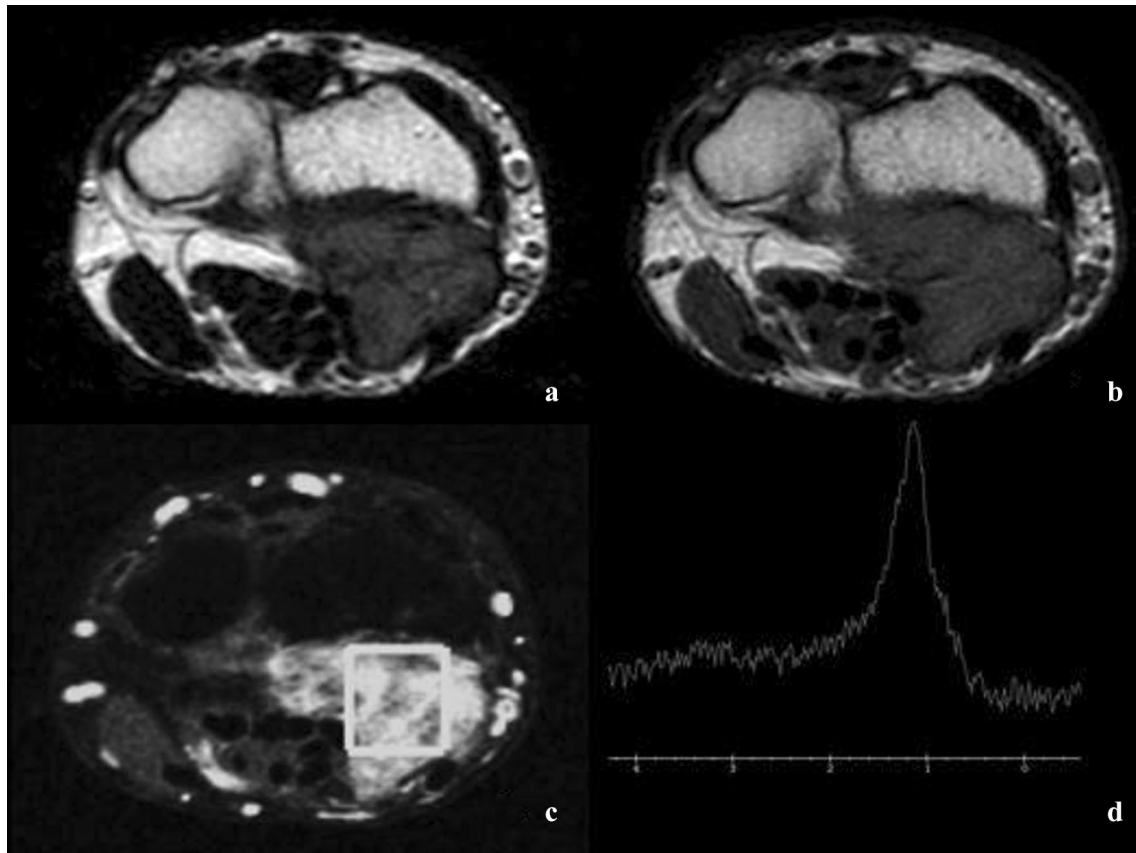


Fig. 3 MRI axial images of a solid lesion at the level of the flexor tendons of the wrist showing a low signal intensity on T1- and T2-weighted sequences (**a**, **b**) and intense contrast enhancement after

gadolinium injection (**c**). The MR spectroscopy analysis after ROI positioning shows a choline peak (**d**). The imaging features are consistent with a giant cell tumor of the tendon sheaths (GCTTS)

positive choline peak, and also a large number of inflammatory lesions may produce a high choline peak [16].

For example, benign *peripheral nerve sheath tumors* typically have detectable choline content by MRS. In a recent study that used MR spectroscopy to evaluate BPNSTs and MPNSTs, trimethylamine concentrations and the trimethylamine fraction were found to be relatively lower in the benign neoplasms, and a trimethylamine fraction threshold of 50% resulted in 100% sensitivity and 72.2% specificity [45].

The presence of a lipid peak can be detected in the wall of abscesses, in the solid part of highly malignant lesions, and in tumors during treatment response, probably related to cell membrane turnover. Lipid peak, however, has to be analyzed carefully, due to the possibility of lipid contamination caused by surrounding tissue [11, 16].

MRS evaluation of choline may be used not only for tumor characterization but also to assess treatment response, showing a choline peak reduction after chemotherapy in malignant musculoskeletal lesions [11].

The limitation of the literature choline MRS studies up to date is that they are mostly qualitative rather than

quantitative, making the distinction of metabolically active benign soft tissue tumors from malignant masses difficult. So, currently, the utility of MRS is limited to its high negative predictive value [29].

Diffusion tensor imaging and tractography

Diffusion tensor imaging (DTI) and tractography are feasible techniques to visualize the spatial anatomy of peripheral nerves in the presence of STT, especially in cases where the course and the involvement of major peripheral nerves are difficult to assess with standard morphological MR sequences [20, 23, 42, 46].

Technique

DTI evaluates the three-dimensional (3D) motion of protons in tissues providing quantitative data on the amount and directionality of random movement of water molecules [46]. Different tissues show specific structural properties that facilitate molecules diffusion in a particular direction while

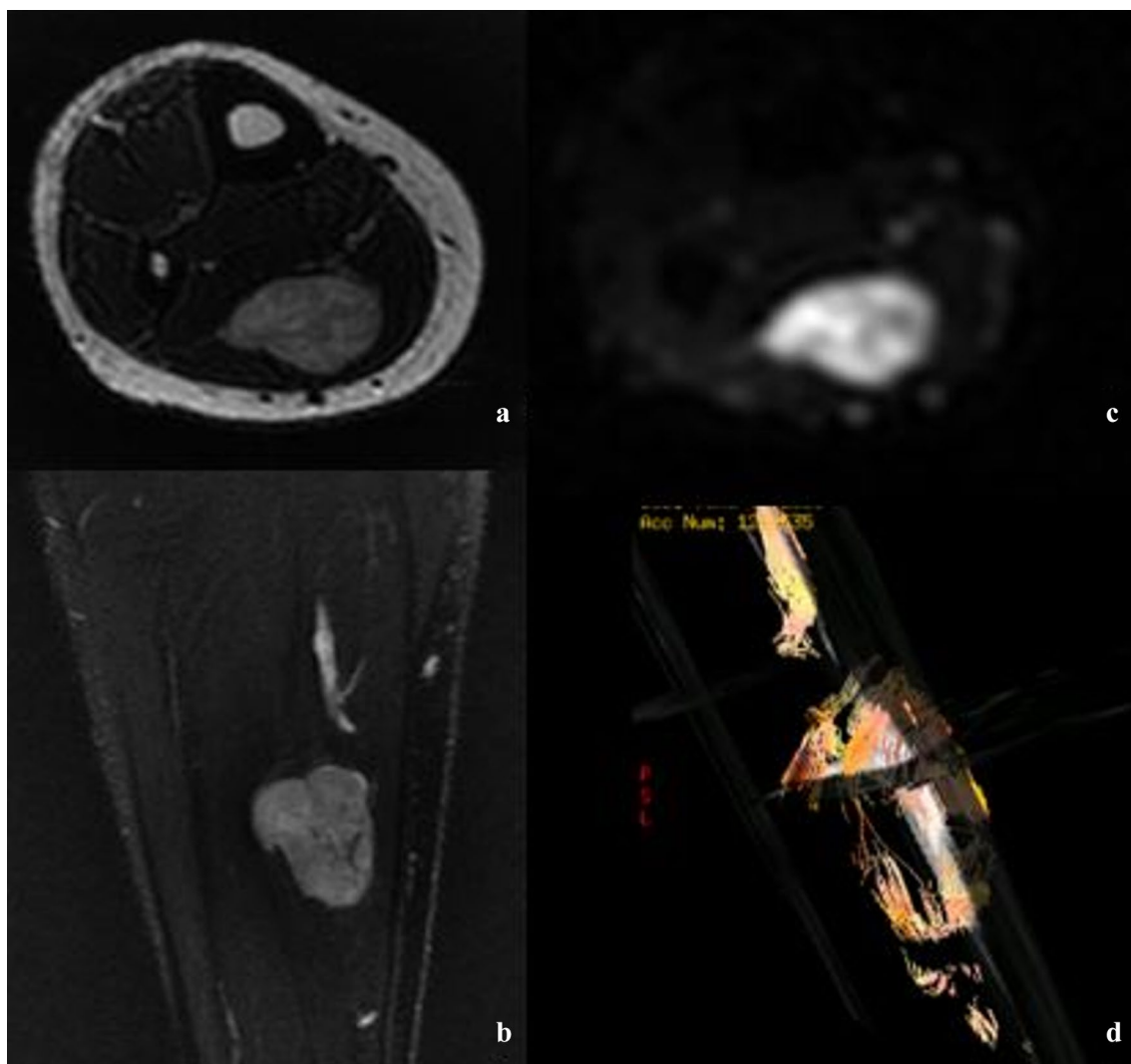


Fig. 4 Axial (a) an coronal (b) MR images of a rounded fusiform lesion at the level of the posterior compartment of the leg (within the soleus muscle) showing intense, homogeneous contrast enhancement. Axial DTI sequence (c) with fiber track reconstruction (d) demon-

strates the growth of the lesion within the nerve fibers and its relationship to them. The imaging features are consistent with the diagnosis of schwannoma

limiting it in another, the so-called anisotropy. In peripheral nerves, due to the presence of nerve fiber fascicles, water molecules tend to move in the direction of the axons (“anisotropic diffusion”). The differences in anisotropic characteristics of different tissues allow DTI to image nerve tracts and surrounding tissues [20]. At our institution, we perform DTT using a 3 Tesla MRI scanner (EPI sequence, three diffusion directions, b value of 1000 s/mm^2). The diffusion is quantified by the apparent diffusion coefficient (ADC), and fractional anisotropy maps with diffusion directions are color coded. High-resolution images are also acquired using morphological sequences. Images are evaluated for image quality, ADC of the lesion, tractography, and fractional anisotropy of nerves.

Applications

In musculoskeletal imaging clinical practice, DTI and tractography are mainly used to evaluate peripheral nerve tumors and soft tissue tumors arising around nerve structures [20]. This approach is of paramount importance not only for the diagnosis when there is often great difficulty in correctly delineating the tumor from healthy nerve structures, but also for the preoperative planning, as the preservation of unaffected nerve fascicles is important to maintain neuromuscular function after surgery [20]. The assessment of peripheral nerve involvement by STTs, based on conventional structural MR sequences alone, is limited by subjective interpretation. Moreover, correlation of “d” sectional images with surgical findings, particularly in anatomically complex regions, can

be challenging [46]. DTI and tractography have radically changed the ability to visualize tissue anatomy in a three-dimensional, noninvasive manner. Using tractography, the topographical relationship between the peripheral nerve and the tumor can be clearly depicted, even in the presence of regional anatomy derangement. In schwannomas, in which the tumor originates from the sheath of a single fascicle, leaving the main trunk of the peripheral nerve attached to the mass, DTI and tractography imaging are helpful in the differential diagnosis with neurofibromas, clearly depicting the eccentric and separate tumor growth relative to the involved nerve. Moreover, in addition to the morphological T2 sequence, discontinuity and abrupt thinning are signs that may indicate nerve invasion. Also, the literature results report a tendency toward lower FA and higher ADC values for adjacent nerve segments in malignant STTs than in benign STTs. These findings could be explained by the presence of greater regional nerve edema associated with aggressive tumor behavior or by true tumoral infiltration [23, 46]. In our experience, DTT was found to be capable of properly visualizing intact nerve fascicles and correctly delineating healthy nerve tissue and tumors across the vast majority of PNST patients with good intraoperative correlation between the DTT scans and surgical anatomy with 95.8% sensitivity, 66.8% specificity, and 89% positive predictive value (Fig. 4).

Conclusions

Functional and metabolic MRI techniques have expanded the role of MRI in the evaluation of soft tissue tumors. The added information obtained from these sequences, either alone or integrated, may improve multiparametric evaluations of soft tissue tumors that result in more accurate diagnosis, appropriate treatment planning, and monitoring of treatment efficacy. It is important to further implement these techniques to be able to use them on a routine clinical basis and to standardize furtherly acquisition protocols.

Compliance with ethical standards

Conflict of interest All authors declare that they have no conflict of interest.

Ethical approval This article does not contain any studies with human participants performed by any of the authors.

References

1. Beaman FD, Jelinek JS, Priebat DA (2013) Current imaging and therapy of malignant soft tissue tumors and tumor-like lesions. *Semin Musculoskelet Radiol* 17:168–176. <https://doi.org/10.1055/s-0033-1343094>
2. Barile A, Conti L, Lanni G et al (2013) Evaluation of medial meniscus tears and meniscal stability: weight-bearing MRI vs arthroscopy. *Eur J Radiol* 82:633–639. <https://doi.org/10.1016/j.ejrad.2012.10.018>
3. Barile A, Lanni G, Conti L et al (2013) Lesions of the biceps pulley as cause of anterosuperior impingement of the shoulder in the athlete: potentials and limits of MR arthrography compared with arthroscopy. *Radiol Med* 118:112–122. <https://doi.org/10.1007/s11547-012-0838-2>
4. Salvati F, Rossi F, Limbucci N et al (2008) Muroid metaplastic degeneration of anterior cruciate ligament. *J Sports Med Phys Fitness* 48:483–487
5. Mariani S, La Marra A, Arrigoni F et al (2015) Dynamic measurement of patello-femoral joint alignment using weight-bearing magnetic resonance imaging (WB-MRI). *Eur J Radiol* 84:2571–2578. <https://doi.org/10.1016/j.ejrad.2015.09.017>
6. Barile A, Bruno F, Mariani S et al (2017) Follow-up of surgical and minimally invasive treatment of Achilles tendon pathology: a brief diagnostic imaging review. *Musculoskelet Surg* 101:51–61. <https://doi.org/10.1007/s12306-017-0456-1>
7. Barile A, Bruno F, Arrigoni F et al (2017) Emergency and trauma of the ankle. *Semin Musculoskelet Radiol* 21:282–289. <https://doi.org/10.1055/s-0037-1602408>
8. Zappia M, Castagna A, Barile A et al (2017) Imaging of the coracoglenoid ligament: a third ligament in the rotator interval of the shoulder. *Skeletal Radiol* 46:1101–1111. <https://doi.org/10.1007/s00256-017-2667-9>
9. Barile A, Arrigoni F, Bruno F et al (2017) Computed tomography and MR imaging in rheumatoid arthritis. *Radiol Clin N Am*. <https://doi.org/10.1016/j.rcl.2017.04.006>
10. Limbucci N, Rossi F, Salvati F et al (2010) Bilateral suprascapular nerve entrapment by glenoid labral cysts associated with rotator cuff damage and posterior instability in an amateur weightlifter. *J Sports Med Phys Fitness* 50:64–67
11. Costa FM, Canella C, Gasparetto E (2011) Advanced magnetic resonance imaging techniques in the evaluation of musculoskeletal tumors. *Radiol Clin N Am* 49:1325–1358. <https://doi.org/10.1016/j.rcl.2011.07.014>
12. Bancroft L, Pettis C, Wasylw C (2013) Imaging of benign soft tissue tumors. *Semin Musculoskelet Radiol* 17:156–167. <https://doi.org/10.1055/s-0033-1343071>
13. Teixeira PAG, Beaumont M, Gabriela H et al (2015) Advanced techniques in musculoskeletal oncology: perfusion, diffusion, and spectroscopy. *Semin Musculoskelet Radiol* 19:463–474. <https://doi.org/10.1055/s-0035-1569250>
14. Masciocchi C, Conti L, D’Orazio F et al (2012) Errors in musculoskeletal MRI. In: *Errors in radiology*. Springer, Italia. https://doi.org/10.1007/978-88-470-2339-0_18
15. Subhawong TK, Jacobs MA, Fayad LM (2014) Insights into quantitative diffusion-weighted MRI for musculoskeletal tumor imaging. *Am J Roentgenol* 203:560–572. <https://doi.org/10.2214/AJR.13.12165>
16. Russo F, Mazzetti S, Grignani G et al (2012) In vivo characterisation of soft tissue tumours by 1.5-T proton MR spectroscopy. *Eur Radiol* 22:1131–1139. <https://doi.org/10.1007/s00330-011-2350-9>
17. Masciocchi C, Lanni G, Conti L et al (2012) Soft-tissue inflammatory myofibroblastic tumors (IMTs) of the limbs: potential and limits of diagnostic imaging. *Skeletal Radiol* 41:643–649. <https://doi.org/10.1007/s00256-011-1263-7>
18. Buchbender C, Heusner TA, Lauenstein TC et al (2012) Oncologic PET/MRI, part 2: bone tumors, soft-tissue tumors, melanoma, and lymphoma. *J Nucl Med* 53:1244–1252. <https://doi.org/10.2967/jnumed.112.109306>

19. Genovese E, Cani A, Rizzo S et al (2011) Comparison between MRI with spin-echo echo-planar diffusion-weighted sequence (DWI) and histology in the diagnosis of soft-tissue tumours. *Radiol Med* 116:644–656. <https://doi.org/10.1007/s11547-011-0666-9>
20. Aszmann OC (2015) Diffusion tensor tractography for the surgical management of peripheral nerve sheath tumors. *Neurosurg Focus* 39:1–6. <https://doi.org/10.3171/2015.6.FOCUS15228>
21. Subhawong TK, Wilky BA (2015) Value added. *Curr Opin Oncol* 27:323–331. <https://doi.org/10.1097/CCO.000000000000199>
22. Drapé JL (2013) Advances in magnetic resonance imaging of musculoskeletal tumours. *Orthop Traumatol Surg Res* 99:S115–S123. <https://doi.org/10.1016/j.otsr.2012.12.005>
23. Soldatos T, Fisher S, Karri S et al (2015) Advanced MR imaging of peripheral nerve sheath tumors including diffusion imaging theodoros. *Semin Musculoskelet Radiol* 19:179–190
24. Van Rijswijk CSP, Kunz P, Hogendoorn PCW et al (2002) Diffusion-weighted MRI in the characterization of soft-tissue tumors. *J Magn Reson Imaging* 15:302–307. <https://doi.org/10.1002/jmri.10061>
25. Pozzi G, Albano D, Messina C et al (2017) Solid bone tumors of the spine: diagnostic performance of apparent diffusion coefficient measured using diffusion-weighted MRI using histology as a reference standard. *J Magn Reson Imaging* 47:1034–1042
26. Dietrich O, Raya JG, Sommer J et al (2005) A comparative evaluation of a RARE-based single-shot pulse sequence for diffusion-weighted MRI of musculoskeletal soft-tissue tumors. *Eur Radiol* 15:772–783. <https://doi.org/10.1007/s00330-004-2619-3>
27. Khoo MMY, Tyler PA, Saifuddin A, Padhani AR (2011) Diffusion-weighted imaging (DWI) in musculoskeletal MRI: a critical review. *Skelet Radiol* 40:665–681
28. Oka K, Yakushiji T, Sato H et al (2011) Usefulness of diffusion-weighted imaging for differentiating between desmoid tumors and malignant soft tissue tumors. *J Magn Reson Imaging* 33:189–193. <https://doi.org/10.1002/jmri.22406>
29. Ahlawat S, Fayad LM (2015) De novo assessment of pediatric musculoskeletal soft tissue tumors: beyond anatomic imaging. *Pediatrics* 136:e194–e202. <https://doi.org/10.1542/peds.2014-2316>
30. Lee SY, Jee WH, Jung JY et al (2016) Differentiation of malignant from benign soft tissue tumours: use of additive qualitative and quantitative diffusion-weighted MR imaging to standard MR imaging at 3.0 T. *Eur Radiol* 26:743–754. <https://doi.org/10.1007/s00330-015-3878-x>
31. Pekcevik Y, Kahya MO, Kaya A (2015) Characterization of soft tissue tumors by diffusion-weighted imaging. *Iran J Radiol* 12:1–6. <https://doi.org/10.5812/iranjradiol.15478v2>
32. Demehri S, Belzberg A, Blakeley J, Fayad LM (2014) Conventional and functional MR imaging of peripheral nerve sheath tumors: initial experience. *Am J Neuroradiol* 35:1615–1620. <https://doi.org/10.3174/ajnr.A3910>
33. Jeon JY, Chung HW, Lee MH, Lee SH, Shin MJ (2016) Usefulness of diffusion-weighted MR imaging for differentiating between benign and malignant superficial soft tissue tumors and tumor-like lesions. *Br Inst Radiol* 89:20150929
34. Oka K, Yakushiji T, Sato H et al (2008) Ability of diffusion-weighted imaging for the differential diagnosis between chronic expanding hematomas and malignant soft tissue tumors. *J Magn Reson Imaging* 28:1195–1200. <https://doi.org/10.1002/jmri.21512>
35. Barile A, Bruno F, Mariani S et al (2017) What can be seen after rotator cuff repair: a brief review of diagnostic imaging findings. *Musculoskelet Surg*. <https://doi.org/10.1007/s12306-017-0455-2>
36. De Filippo M, Pesce A, Barile A et al (2017) Imaging of postoperative shoulder instability. *Musculoskelet Surg* 101:15–22
37. Barile A, Regis G, Masi R et al (2007) Patologia neoplastica muscoloscheletrica: esperienza preliminare con RM perfusionale. *Radiol Med* 112:550–561. <https://doi.org/10.1007/s11547-007-0161-5>
38. Park MY, Jee W-H, Kim SK et al (2013) Preliminary experience using dynamic MRI at 3.0 Tesla for evaluation of soft tissue tumors. *Korean J Radiol* 14:102–109. <https://doi.org/10.3348/kjr.2013.14.1.102>
39. Barile A, Sabatini M, Iannesi F et al (2004) Pigmented villonodular synovitis (PVNS) of the knee joint: magnetic resonance imaging (MRI) using standard and dynamic paramagnetic contrast media. Report of 52 cases surgically and histologically controlled. *Radiol Med* 107:356–366
40. van Rijswijk CSP, Geirnaerdt MJA, Hogendoorn PCW et al (2004) Soft-tissue tumors: value of static and dynamic gadopentetate dimeglumine-enhanced MR imaging in prediction of malignancy. *Radiology* 233:493–502. <https://doi.org/10.1148/radiol.2332031110>
41. Zoccali C, Rossi B, Zoccali G et al (2015) A new technique for biopsy of soft tissue neoplasms: a preliminary experience using MRI to evaluate bleeding. *Minerva Med* 106:117–120
42. Liu X, Ekholm S, Tian W, et al (2006) Preliminary application study of MR perfusion imaging and diffusion tensor imaging in tumor like lesions in the cervical spinal cord. In: *Proceedings 14th scientific meeting international society for magnetic resonance in medicine*, p 985
43. Moukaddam H, Pollak J, Haims AH (2009) MRI characteristics and classification of peripheral vascular malformations and tumors. *Skelet Radiol* 38:535–547. <https://doi.org/10.1007/s00256-008-0609-2>
44. Fayad L, Deshmukh S, Subhawong T, Carrino J (2014) Role of MR spectroscopy in musculoskeletal imaging. *Indian J Radiol Imaging* 24:210. <https://doi.org/10.4103/0971-3026.137024>
45. Thawait GK, Subhawong TK, Tatizawa Shiga NY, Fayad LM (2014) “Cystic”-appearing soft tissue masses: what is the role of anatomic, functional, and metabolic MR imaging techniques in their characterization? *J Magn Reson Imaging* 39:504–511. <https://doi.org/10.1002/jmri.24314>
46. Kasprian G, Amann G, Panotopoulos J et al (2015) Peripheral nerve tractography in soft tissue tumors: a preliminary 3-tesla diffusion tensor magnetic resonance imaging study. *Muscle Nerve* 51:338–345. <https://doi.org/10.1002/mus.24313>

Publisher's Note Springer Nature remains neutral with regard to jurisdictional claims in published maps and institutional affiliations.